

Compositional stability of sediment microbial communities during a seagrass meadow decline

Marsej Markovski¹, Mirjana Najdek¹, Gerhard J. Herndl^{2,3}, and Marino Korlević^{1*}

1. Center for Marine Research, Ruđer Bošković Institute, Croatia

2. Department of Functional and Evolutionary Ecology, University of Vienna, Austria

3. Department of Marine Microbiology and Biogeochemistry, Royal Netherlands Institute for Sea
Research (NIOZ), Utrecht University, The Netherlands

*To whom correspondence should be addressed:

Marino Korlević

G. Paliaga 5, 52210 Rovinj, Croatia

Tel.: +385 52 804 768

Fax: +385 52 804 780

e-mail: marino.korlevic@irb.hr

Running title: Compositional stability of sediment communities

1 Abstract

2 The presence of seagrass shapes surface sediments and forms a specific environment for
3 diverse and abundant microbial communities. A severe decline of *Cymodocea nodosa*, a widespread
4 seagrass species in the Mediterranean Sea, has been documented. To characterise and assess the
5 changes in microbial community composition during the decline of a *Cymodocea nodosa* meadow,
6 Illumina MiSeq sequencing of the V4 region of the 16S rRNA gene was performed. Samples of
7 surface sediments were collected at monthly intervals from July 2017 to October 2018. Samples
8 from an adjacent, nonvegetated site were also analysed for comparison. Microbial communities
9 were stratified by sediment depth and differed between the vegetated and the nonvegetated site.
10 Although the *C. nodosa* meadow declined to a point where almost no leaves were present, no clear
11 temporal succession in the community was observed. Taxonomic analysis revealed a dominance
12 of bacterial over archaeal sequences, with most archaeal reads classified as *Nanoarchaeota*,
13 *Thermoplasmatota*, *Crenarchaeota*, and *Asgardarchaeota*. The bacterial community was mainly
14 composed of *Desulfobacterota*, *Gammaproteobacteria*, *Bacteroidota*, *Chloroflexi*, *Planctomycetota*,
15 and *Campylobacterota*. Our results show that sediment microbial communities are remarkably
16 stable and may resist major disturbances such as seagrass meadow decline.

17 **Introduction**

18 Shallow coastal sediments are often colonized by seagrasses, which cover approximately 0.1
19 to 0.2 % of the global ocean (Duarte, 2002). Seagrasses penetrate the sediment with their roots and
20 rhizomes forming extensive meadows. The presence of seagrass meadows shapes surface sediments
21 and provides a specific environment for diverse and abundant microbial communities (Duarte et al.,
22 2005). Sediments colonized by seagrasses are considered hotspots for microbial activity as seagrass
23 meadows enrich the underlying sediment with organic matter (Duarte et al., 2005). High organic
24 matter content is mainly achieved by releasing dissolved organic carbon from seagrass roots and by
25 trapping organic particles from the water column (Duarte, 2002). Moreover, seagrasses stabilize the
26 underlying sediment, promoting the accumulation of organic matter and sediment particles (Fonseca
27 and Kenworthy, 1987; Terrados and Duarte, 2000; van Katwijk et al., 2010). In addition, seagrass
28 beds can also increase the availability of organic matter indirectly through the decomposition of
29 detached leaves, roots and rhizomes (Jensen et al., 2007; Liu et al., 2017).

30 Studies of marine sediment microbial communities primarily focus on changes in microbial
31 abundance and activity with sediment depth (Jørgensen and Marshall, 2016; Petro et al., 2017;
32 Starnawski et al., 2017; Orsi, 2018). Depth-dependent changes in taxonomic composition have been
33 well described differentiating surface sediment communities dominated by *Bacteria*, especially
34 *Proteobacteria*, from deeper communities characterized by *Archaea* (Orcutt et al., 2011; Chen et al.,
35 2017; Petro et al., 2017). Coastal surface sediments colonized by seagrass are not as well investigated
36 due to studies focusing primarily on rhizosphere communities and only occasionally including
37 sediment communities for comparison (Cúcio et al., 2016; Rabbani et al., 2021). Communities
38 in the rhizosphere are species-specific and differ from those in the sediment. One of the main
39 differences is the higher relative abundance of *Desulfobacterota*, one of the most abundant sulphate
40 reducing bacteria in seagrass sediments, in contrast to the rhizosphere, which is characterized
41 by *Epsilonproteobacteria* (Ettinger et al., 2017). When sediment microbial communities were
42 described, the main focus was on the differences between vegetated and nonvegetated sites (Zheng

et al., 2019; Sun et al., 2020). In addition, these studies showed that communities differ even with respect to the meadow edge (Ettinger et al., 2017). However, little is known about the response of these communities to seagrass decline. Only limited information is available on the succession of microbial communities in seagrass sediments including the dynamics and activity of sulphate-reducing prokaryotes (Smith et al., 2004), the response of microbial communities to nutrient enrichment (Guevara et al., 2014), and community changes associated with seagrass restoration (Bourque et al., 2015). These studies suggest that seagrass decline may trigger changes in the sediment communities.

In the Mediterranean Sea, *Cymodocea nodosa* is a widespread seagrass species declining in coastal areas (Ruiz Fernandez et al., 2009; Tuya et al., 2014; Orlando-Bonaca et al., 2015). The rhizosphere and epiphytic communities of *C. nodosa* have been described (Cúcio et al., 2016; Korlević et al., 2021a), however, little is known about sediment communities underlying *C. nodosa* meadows. The aim of the present study was to characterize the taxonomic composition of sediment communities of a *C. nodosa* meadow and to assess the temporal dynamics of these communities. As the studied meadow experienced a major decline (Najdek et al., 2020), we investigated whether this event affected the sediment microbial community structure.

59 **Materials and methods**

60 **Sampling**

61 Sediment cores were sampled in a declining *C. nodosa* meadow (vegetated site) located in the
62 Bay of Saline, east coast of the northern Adriatic Sea (45°7'5'' N, 13°37'20'' E) (Figure 1). Cores
63 were collected monthly from July 2017 to October 2018 (Supplementary Table S1) by diving using
64 15 cm long plastic core samplers. Sediment samples were immediately transported on ice to the
65 laboratory and stored at -80 °C until further processing. The adjacent nonvegetated area was also
66 sampled for comparison (Figure 1). A detailed description of the study site, the decline of the *C.*
67 *nodosa* meadow and the dynamics of environmental conditions during the decline are provided in
68 Najdek et al. (2020).

69 **DNA isolation**

70 Total DNA from sediment samples was extracted following a modified (Pjevac et al., 2018)
71 isolation protocol of Zhou et al. (1996). Prior to DNA isolation, cores were cut into four different
72 1 cm sections: top (0 – 1 cm), bottom (7 – 8 cm), and two middle sections: upper middle (1 – 3
73 cm) and lower middle (3 – 6 cm) section. Sediment samples were weighted (2 g) avoiding roots
74 and rhizomes from vegetated cores, mixed with 5.4 ml of extraction buffer (100 mM Tris [pH 8.0],
75 100 mM sodium EDTA [pH 8.0], 100 mM Na₃PO₄ [pH 8.0], 1.5 M NaCl, 1 % CTAB) and 10 µl
76 of proteinase K (20 mg ml⁻¹) and incubated by horizontal shaking at 225 rpm at 37°C for 30 min.
77 Thereafter 1.2 ml of 10 % SDS was added and the mixture incubated again by horizontal shaking at
78 225 rpm at 65°C for 60 min. The supernatant was collected after centrifugation at 3220 × g at room
79 temperature for 10 min and mixed with an equal volume of chloroform:isoamyl alcohol (1:1). The
80 aqueous phase was retrieved after centrifugation at 3220 × g at room temperature for 10 min. The
81 extraction procedure with the organic solvent mixture was repeated twice. After the final extraction

82 0.6 volumes of isopropanol were added to precipitate the DNA. The mixture was incubated at 22°C
83 for 60 min and centrifuged at 3220 × g at room temperature for 45 min. The obtained pellet was
84 washed twice with 10 ml of chilled 70 % ethanol, centrifuged at 3220 × g at room temperature for
85 10 min after each washing, and finally resuspended in 100 µl of deionized water.

86 **Illumina 16S rRNA sequencing**

87 The V4 region of the 16S rRNA gene was sequenced using a two-step PCR approach
88 described previously (Korlević et al., 2021b). Briefly, the V4 region was amplified using the 515F
89 (5'-GTGYCAGCMGCCGCGTAA-3') and 806R (5'-GGACTACNVGGGTWTCTAAT-3') primers
90 from the Earth microbiome project (<https://earthmicrobiome.org/protocols-and-standards/16s/>),
91 which contained a sequence tag on the 5' end (Caporaso et al., 2011, 2012; Apprill et al., 2015;
92 Parada et al., 2016). Purified samples were sent for Illumina MiSeq sequencing (2 × 250 bp) at
93 IMGM Laboratories (Martinsried, Germany) where the second PCR of the two-step PCR approach
94 was performed using primers targeting the tag region incorporated in the first PCR. These primers
95 also contained adapter and sample-specific index sequences. For each sequencing batch, a positive
96 and a negative control were also sequenced. The positive control consisted of a mock community
97 composed of uniformly mixed DNA from 20 different bacterial strains (ATCC MSA-1002, ATCC,
98 USA), while PCR reactions without DNA template served as the negative control. Sequences
99 obtained in this study have been deposited in the European Nucleotide Archive at EMBL-EBI under
100 the accession numbers SAMEA11293274 – SAMEA11293412 and SAMEA6648825.

101 **Sequence and data analysis**

102 Sequences were analysed on the computer cluster Isabella (University Computing Center,
103 University of Zagreb) using version 1.45.2 of mothur (Schloss et al., 2009) according to the MiSeq
104 Standard Operating Procedure (MiSeq SOP; https://mothur.org/wiki/miseq_sop/) (Kozich et al.,

105 2013) and recommendations given by the Riffomonas project (<https://riffomonas.org>) to foster data
106 reproducibility. Alignment and classification were performed using the 138.1 release of the SILVA
107 SSU Ref NR 99 database (<https://www.arb-silva.de>) (Quast et al., 2013; Yilmaz et al., 2014). A
108 cut-off of 97 % was used to cluster sequences into operational taxonomic units (OTUs).

109 Pipeline data processing and visualization were done using R (version 3.6.3) (R Core Team,
110 2020) combined with packages vegan (version 2.5.7) (Oksanen et al., 2020) tidyverse (version
111 1.3.1) (Wickham et al., 2019) and multiple other packages (Neuwirth, 2014; Xie, 2014, 2015, 2019,
112 2021a, 2021b; Xie et al., 2018, 2020; Edwards, 2020; Wilke, 2020; Allaire et al., 2021; Zhu, 2021).
113 Observed number of OTUs, Chao1, ACE, exponential of the Shannon diversity index and Inverse
114 Simpson diversity index were calculated after normalization to the minimum number of reads per
115 sample to account for different sequencing depths using vegan's function **rrarefy** (Oksanen et
116 al., 2020). Chao1 and ACE estimators were calculated using vegan's function **estimateR**, while
117 Shannon and Inverse Simpson diversity indices were obtained using vegan's function **diversity**
118 (Oksanen et al., 2020). To express both diversity indices in terms of effective number of OTUs the
119 exponential of the Shannon diversity index was retrieved (Jost, 2006). The proportions of shared
120 community members between different sediment layers and the two sites were expressed as the
121 Bray-Curtis similarity coefficient calculated on the OTU data table using vegan's function **vegdist**
122 and transformed from dissimilarities to similarities (Legendre and Legendre, 2012; Borcard et
123 al., 2018; Oksanen et al., 2020). The Principal Coordinate Analysis (PCoA) was performed on
124 Bray-Curtis dissimilarities based on OTU abundances using the function **wcmdscale** (Legendre and
125 Legendre, 2012; Oksanen et al., 2020). Differences between communities of different layers, sites,
126 years, and decay periods were tested by performing the Analysis of Similarities (ANOSIM) using
127 vegan's function **anosim** and 1000 permutations (Oksanen et al., 2020). In addition, differences
128 between richness estimators, diversity indices, and relative sequence abundances were tested by
129 performing the Mann-Whitney *U* test (function **wilcox.test**), when two groups were compared,
130 or the Kruskal-Wallis *H* test (function **kruskal.test**) followed by a pairwise comparison using
131 the Mann-Whitney *U* test (function **pairwise.wilcox.test**), when more than two groups were

¹³² compared. Bonferroni correction was applied to address the problem of multiple comparisons.

¹³³ In total 3.3 million sequences were obtained after quality curation and exclusion of
¹³⁴ sequences without known relatives (no relative sequences), and eukaryotic, chloroplast, and
¹³⁵ mitochondrial sequences. Altogether, 68 samples from the vegetated sediment and 68 from the
¹³⁶ nonvegetated sediment were analysed. The number of reads per sample ranged from 9,722 to 55,381
¹³⁷ (Supplementary Table S1). Even with the highest sequencing effort the rarefaction curves did not
¹³⁸ level off as commonly observed in high-throughput 16S rRNA amplicon sequencing approaches
¹³⁹ (Supplementary Figure S1, and S2). After quality curation and exclusion of sequences as mentioned
¹⁴⁰ above, reads were clustered into 89,488 different OTUs. Normalization to the minimum number of
¹⁴¹ sequences (9,722) described earlier resulted in 64,335 distinct OTUs ranging from 1,774 to 3,576
¹⁴² OTUs per sample (Supplementary Figure S3). Based on the positive control, a sequencing error
¹⁴³ rate of 0.01 % was calculated which is in line with previously reported values for high-throughput
¹⁴⁴ sequencing data (Kozich et al., 2013; Schloss et al., 2016). Following quality curation, the negative
¹⁴⁵ controls yielded on average 34.2 ± 62.6 sequences. The detailed analysis procedure is available in a
¹⁴⁶ Github repository (https://github.com/MicrobesRovinj/Markovski_SalineSediment16S_x_2022).

147 **Results**

148 To assess the richness and diversity of microbial communities in sediments of the Bay of
149 Saline the observed number of OTUs, Chao1, ACE, exponential of the Shannon diversity index, and
150 Inverse Simpson diversity index were calculated (Figure 2). The observed number of OTUs was
151 similar between the vegetated ($2,746.7 \pm 398.4$ OTUs) and the nonvegetated sediment ($2,883.0 \pm$
152 353.1 OTUs) and showed no statistical difference ($p = 0.06$). Interestingly, both the highest and
153 lowest number of OTUs were observed in the vegetated sediment, more specifically the highest
154 number was found in the top layer ($2,976.1 \pm 262.0$ OTUs) and lowest in the bottom layer ($2,500.4$
155 ± 462.7 OTUs). These layers were also the only ones showing statistical difference in the vegetated
156 site (Figure 2 and Supplementary Table S2). In contrast, the observed number of OTUs in the
157 nonvegetated sediment was similar across sediment layers and did not show significant differences
158 (Figure 2 and Supplementary Table S3), although the lowest value was also observed in the bottom
159 layer ($2,700.8 \pm 378.8$ OTUs). During the study period, the observed number of OTUs was variable,
160 with no clear temporal trend observed (Supplementary Figure S3). Chao1, ACE, exponential of
161 the Shannon diversity index and the Inverse Simpson diversity index of sediment communities
162 in the site with and without vegetation were very similar, with no estimate or index showing a
163 statistically significant difference (all $p > 0.1$). In addition, the Chao1 and ACE richness estimators
164 also showed no significant differences between sediment layers (Figure 2 and Supplementary Tables
165 S2 and S3). In contrast, diversity indices in the vegetated sediment showed a difference between
166 the top and bottom layer and between the upper middle and bottom layer, with exponential of the
167 Shannon diversity index also showing a significant difference between the top and lower middle
168 layer (Figure 2 and Supplementary Table S2). In the nonvegetated sediment, the different sediment
169 layers showed no statistical difference in either richness or diversity (Figure 2 and Supplementary
170 Table S3). Temporal variability in richness estimates and diversity indices was high in both sites,
171 with no clear trend (Supplementary Figures S3 and S4).

172 To evaluate the dynamics of sediment microbial communities Principal Coordinate Analyses

(PCoA) of Bray-Curtis distances based on OTU community data were performed. PCoA of all samples differentiated communities based on sediment depth along the first axis, whereas samples from the vegetated and nonvegetated site were separated along the second axis (Figure 3). ANOSIM confirmed that sediment communities in the Bay of Saline differed between sediment layers with some overlap ($R = 0.48, p < 0.001$), while the communities of the vegetated and nonvegetated site showed a higher degree of overlap ($R = 0.27, p < 0.001$). When communities of different sediment layers were analysed separately, a clearer differentiation between communities of the vegetated and nonvegetated site was observed ($R = 0.45 – 0.49$, all $p < 0.001$). Interestingly, when samples from the same layer of the vegetated and nonvegetated site were compared, the top layers of the sediment showed the highest degree of similarity (Bray-Curtis, 0.64), while the lowest degree of similarity was observed in samples from the upper middle and bottom layers (Bray-Curtis, 0.59) (Figure 3 and Supplementary Figure S5). When samples from each site were analysed separately, the previously observed differentiation of samples based on sediment depth was noted (Figure 4) (ANOSIM; vegetated, $R = 0.50, p < 0.001$ and nonvegetated $R = 0.49, p < 0.001$) with the highest degree of similarity observed between samples from middle layers (Bray-Curtis; vegetated, 0.71 and nonvegetated, 0.71) and between lower middle and bottom layers (Bray-Curtis; vegetated, 0.69 and nonvegetated, 0.71) (Supplementary Figure S5). To determine whether there is a temporal succession in the community pattern, samples from each layer and site were analysed separately to exclude the effects of sediment depth and vegetation, which have been shown to primarily influence sediment community structure (Figure 4). No grouping of samples by month was observed in any of the layers and sites analysed. Although Najdek et al. (2020) described a sharp decline in aboveground biomass in the same meadow since the beginning of 2018, we did not detect a clearly defined grouping of samples based on sampling year in all the analysed layers (ANOSIM; vegetated, $R = 0.06 – 0.26, p = 0.05 – 0.18$ and nonvegetated, $R = 0.03 – 0.18 p = 0.05 – 0.29$). In addition, we also analysed the samples according to the reported decline of roots and rhizomes, as belowground biomass showed a later onset of decline than the aboveground biomass (Najdek et al., 2020). However, this analysis also did not reveal a grouping in any of the tested layers (ANOSIM;

200 vegetated, $R = 0.07 - 0.19$, $p = 0.05 - 0.18$ and nonvegetated, $R = 0.16 - 0.20$, $p = 0.05 - 0.06$).
201 Furthermore, as with the community analysis, taxonomic classification of all samples also did not
202 indicate a temporal succession but a fairly stable community composition was detected in all layers
203 both in the vegetated and nonvegetated site (Supplementary Figure S6).

204 Archaeal sequences comprised $9.5 \pm 4.7\%$ of all reads. Sequences classified as *Archaea*
205 increased in relative abundance from the top ($4.5 \pm 1.6\%$) to the bottom sediment layer ($14.1 \pm 4.0\%$). The archaeal community was comprised of *Nanoarchaeota*, *Thermoplasmatota*, *Crenarchaeota*,
206 and *Asgardarchaeota* (Figure 5). *Nanoarchaeota* comprised $3.6 \pm 1.3\%$ of all sequences and were
207 evenly distributed across the different sediment layers, whereas all other archaeal phyla showed a
208 depth-related pattern. All *Nanoarchaeota* related sequences were classified as *Woesearchaeales*,
209 with $28.2 \pm 13.5\%$ of sequences further classified as SCGC AAA011-D5. A particularly pronounced
210 depth-related pattern was found in *Thermoplasmatota*. Sequences classified as *Thermoplasmatota*
211 comprised $4.1 \pm 1.2\%$ of all sequences in the bottom sediment layer and only $0.7 \pm 0.6\%$ in the
212 top layer. The majority of sequences related to this group was further classified as Marine Benthic
213 Group D and DHVEG-1. *Crenarchaeota* comprised $1.8 \pm 2.3\%$ of all reads. This group had a
214 higher relative sequence abundance at the nonvegetated ($2.7 \pm 2.8\%$) than at the vegetated site ($1.0 \pm 0.9\%$) ($p < 0.0001$). The vast majority of *Crenarchaeota* related sequences were classified as
215 *Bathyarcheia*. Out of all reads, *Asgardarchaeota* comprised $0.9 \pm 0.7\%$ of sequences that could all
216 be further classified as *Lokiarchaeia*.

217 Overall, bacterial sequences ($90.5 \pm 4.7\%$) dominated over archaeal ones and were mainly
218 comprised of *Desulfobacterota*, *Gammaproteobacteria*, *Bacteroidota*, *Chloroflexi*, *Planctomycetota*,
219 and *Campylobacterota* (Figure 5). Of all reads, *Desulfobacterota* was the most abundant taxon
220 in the middle (upper middle, $19.4 \pm 2.0\%$ and lower middle, $20.2 \pm 3.2\%$) and bottom layers
221 ($18.3 \pm 3.1\%$) (Figures 5 and 6). *Desulfobacterota* consisted mainly of *Desulfosarcinaceae*,
222 *Desulfatiglandaceae*, *Desulfocapsaceae*, *Desulfobulbaceae*, and uncultured members of the
223 order *Syntrophobacteriales* (Figure 6). Sequences classified as *Desulfocapsaceae* showed affinity
224 to the *Desulfocapsaceae* family of the *Desulfobacterota* (Figure 6). Sequences classified as
225 *Desulfocapsaceae* showed affinity to the *Desulfocapsaceae* family of the *Desulfobacterota* (Figure 6).

226 for the top sediment layer, where they comprised $26.3 \pm 8.2\%$ of *Desulfobacterota* reads
227 compared to the bottom layer where they constituted only $3.8 \pm 3.3\%$ of *Desulfobacterota* reads.
228 *Desulfosarcinaceae* and *Desulfobulbaceae* varied depending on the site. In the whole microbial
229 community, *Desulfosarcinaceae* reads were more abundant at the vegetated ($8.6 \pm 2.7\%$) than
230 nonvegetated site ($6.1 \pm 2.7\%$) ($p < 0.0001$), while sequences classified as *Desulfobulbaceae* were
231 less represented in the vegetated ($0.8 \pm 0.7\%$) than in the nonvegetated sediment ($1.3 \pm 0.7\%$) ($p <$
232 0.0001).

233 *Gammaproteobacteria* comprised most of the *Proteobacteria* sequences ($87.6 \pm 4.1\%$) and
234 made up the majority of all reads in the top sediment layer ($23.2 \pm 6.2\%$) (Figures 5 and 6).
235 This group was represented with more sequences at the nonvegetated ($14.8 \pm 8.9\%$) than at the
236 vegetated site ($9.5 \pm 7.4\%$) ($p < 0.001$). Out of all gammaproteobacterial sequences, 25.2 ± 8.3
237 % of reads could not be further classified than to the class *Gammaproteobacteria* (Figure 6).
238 Sequences that could be further classified were mainly assigned to *Thiotrichaceae*, B2M28,
239 *Woeseiaceae*, *Halieaceae* and *Thioalkalispiraceae* (Figure 6). The observed difference between
240 the relative abundance in *Gammaproteobacteria* at the two sites was particularly pronounced for
241 *Thioalkalispiraceae*. Sequences of this group were more abundant at the nonvegetated ($1.1 \pm 0.8\%$)
242 than at the vegetated site ($0.3 \pm 0.3\%$) ($p < 0.0001$).

243 Sequences classified as *Bacteroidota* were more abundant in the top sediment layer (16.9 ± 2.7
244 %) with their relative abundance decreasing with sediment depth and reaching a minimum in the
245 bottom layer ($6.7 \pm 2.2\%$) (Figures 5 and 6). A higher relative abundance of *Bacteroidota* sequences
246 was observed in the vegetated sediment ($12.0 \pm 4.5\%$) than in the nonvegetated sediment (9.8 ± 4.6
247 %) ($p < 0.01$). *Bacteroidota* were mainly composed of sequences without known relatives within
248 *Bacteroidales*, *Bacteroidetes* BD2-2, *Cyclobacteriaceae*, *Flavobacteriaceae*, *Prolixibacteraceae* and
249 *Saprospiraceae* (Figure 6). In contrast to *Bacteroidota*, sequences classified as *Chloroflexi* increased
250 with sediment depth (top layer, $4.8 \pm 2.0\%$ and bottom layer, $13.8 \pm 2.7\%$) (Figures 5 and 7).
251 *Chloroflexi* were mainly composed of *Anaerolineaceae*, while SBR1031, uncultured *Anaerolineae*,

²⁵² sequences without known relatives within *Anaerolineae* and *Dehalococcoidia*, AB-539-J10, and
²⁵³ *Ktedonobacteraceae* made up the remainder of the *Chloroflexi* community (Figure 7).

²⁵⁴ *Planctomycetota* were evenly represented in the middle (upper middle, $7.3 \pm 0.9\%$ and lower
²⁵⁵ middle, $7.6 \pm 0.9\%$) and bottom layers ($7.5 \pm 1.0\%$), and less abundant in the top layer (6.0 ± 0.7
²⁵⁶ %), showing no difference between the sites (vegetated, $7.0 \pm 1.2\%$ and nonvegetated, 7.1 ± 1.0
²⁵⁷ %) (Figures 5 and 7). The *Planctomycetota* community consisted mainly of SG8-4, *Pirellulaceae*,
²⁵⁸ 4572-13, and sequences that could not be further classified (no relative *Planctomycetota*) (Figure 7).
²⁵⁹ A high proportion of *Planctomycetota* reads ($39.1 \pm 5.1\%$) were assigned to other *Planctomycetota*,
²⁶⁰ indicating a high diversity within this group. *Campylobacterota* comprised on average 3.1 ± 3.0
²⁶¹ % of all sequences (Figures 5 and 7). Overall, no pattern related to sediment depth was observed
²⁶² for this group. Slightly higher values were characteristic for the vegetated ($3.9 \pm 3.5\%$) than the
²⁶³ nonvegetated sediment ($2.3 \pm 2.3\%$) ($p < 0.001$). When differences between sites were tested for
²⁶⁴ all sediment layers, only the difference in the top layer between the two sites (vegetated, 3.4 ± 1.8
²⁶⁵ % and nonvegetated, $1.5 \pm 1.6\%$) was significant ($p < 0.01$). Reads related to *Campylobacterota*
²⁶⁶ could be further classified into two families, *Sulfurimonadaceae* and *Sulfurovaceae* (Figure 7). Of
²⁶⁷ these two families, *Sulfurimonadaceae* showed an area-related difference in relative abundance.
²⁶⁸ Higher values were found at the vegetated ($2.3 \pm 3.4\%$) than at the nonvegetated site (0.7 ± 1.8
²⁶⁹ %) ($p < 0.0001$). *Sulfurimonadaceae* consisted of the genus *Sulfurimonas*, while *Sulfurovaceae*
²⁷⁰ consisted of the genus *Sulfurovum*.

271 **Discussion**

272 Sediments of seagrass meadows harbour diverse, abundant, and active microbial communities
273 (Smith et al., 2004; Duarte et al., 2005; Sun et al., 2015). Although research on microbial
274 communities of seagrass meadows mainly focused on rhizosphere communities, some studies
275 also included the underlying and surrounding sediment (Jensen et al., 2007; Cúcio et al., 2016;
276 Zhang et al., 2020). As with most sediments, a vertical structuring has been found in the microbial
277 communities of seagrass meadow sediments (Sun et al., 2020). Furthermore, a difference between
278 prokaryotic communities of seagrass meadow sediments and nonvegetated sediments has been
279 observed (Ettinger et al., 2017; Zheng et al., 2019). Temporal studies of these communities are
280 generally rare, and little is known about how microbial communities in seagrass meadow sediments
281 change with meadow decline and loss. In this study, we assessed the microbial communities in the
282 sediment of a declining *C. nodosa* meadow to gain further insights into the taxonomic composition,
283 vertical structuring, and dynamics of microbial communities in seagrass meadow sediments.

284 Shannon and Simpson indices account for both richness and evenness and are less sensitive to
285 rare taxa than richness estimators such as ACE and Chao1 (Bent and Forney, 2008). We found no
286 difference in richness (Chao1 and ACE) between sediment layers, suggesting that rare taxa did not
287 play a key role in the vertical structuring of the sediment community in the Bay of Saline (Figure 2).
288 In contrast, diversity indices at the vegetated site showed a depth related pattern (Figure 2). Diversity
289 was highest in the first centimetre of the sediment and differed from the deepest layer (7 – 8 cm).
290 This is consistent with previous studies of marine sediments that describe a decrease in community
291 diversity from the surface to deeper sediment layers, even at small scales within the first few meters
292 (Petro et al., 2017; Hoshino et al., 2020). Seagrasses are known to stabilize the sediment and reduce
293 sediment resuspension (Terrados and Duarte, 2000; van Katwijk et al., 2010). It is possible that
294 the presence of the seagrass, especially roots and rhizomes, increase diversity differences between
295 the top and bottom layer by stabilizing the sediment. In addition, seagrass meadows increase the
296 organic matter content of the sediment through the decay of dead tissue (Jensen et al., 2007; Liu

297 et al., 2017), which may have further contributed to the observed differences between sediment
298 layers. Vertical structuring of sediment communities is typically achieved through burial, which is
299 accompanied by selection based on successive changes in environmental conditions (Petro et al.,
300 2017; Kirkpatrick et al., 2019; Marshall et al., 2019). Specific environmental conditions surrounding
301 roots and rhizomes may act as a filter during burial, separating the top from the bottom layer. In
302 contrast, the sediment of the nonvegetated site remained vertically more stable in terms of richness
303 and diversity.

304 Another component known to differentiate communities in marine sediments besides depth
305 stratification is site-specificity (Polymenakou et al., 2005; Hamdan et al., 2013), which is even
306 more pronounced in seagrass meadows where sediment microbial communities differ not only
307 between the vegetated and nonvegetated area, but also towards the edge of the seagrass patch
308 (Ettinger et al., 2017). In this study, we also observed a grouping of samples according to the
309 two sites (Figure 3), while the microbial communities of both the vegetated and nonvegetated site
310 were stratified according to sediment depth. This is in line with Sun et al. (2020) who noted that
311 the seagrass *Zostera marina* and *Zostera japonica* influence the vertical organisation of microbial
312 communities in the sediment. Although the microbial communities at the vegetated site were distinct
313 from the ones at the nonvegetated site, a high degree of overlap was present. Given that the two
314 sampling sites were in close proximity to each other, a high degree of similarity is not surprising.
315 The microbial communities in the Bay of Saline most likely originate from the same source and
316 only through burial undergo a specific selection characteristic for each site. This type of community
317 structuring (Hamdan et al., 2013; Walsh et al., 2016; Petro et al., 2019) is further supported by
318 the highest degree of similarity between the vegetated and nonvegetated site observed in the top
319 sediment layer. To assess the temporal dynamics of the microbial community, we analysed each
320 sediment layer and site separately to exclude the influence of sediment depth and site-specificity.
321 Because microbial communities of surface sediments have shorter generation times and higher
322 biomass than communities at deeper sediment strata, and seagrass meadow sediments are hotspots
323 for microbial activity (Duarte et al., 2005; Starnawski et al., 2017), successional changes during the

324 decline of a seagrass meadow could be expected. Surprisingly, the decline of the *C. nodosa* meadow
325 in the Bay of Saline appeared to have little or no effect on the microbial community, as we did not
326 observe any grouping of communities according to month, year, or meadow condition (Figure 4). In
327 addition, no temporal patterns were observed in the taxonomic composition, richness, or diversity
328 of the microbial community. Such a stable community structure despite changing environmental
329 conditions (Najdek et al., 2020) could be explained by a greater proportion of dormant or dead
330 microbial cells remaining in the sediment, leading to a perceived taxonomic stability (Luna et al.,
331 2002; Jones and Lennon, 2010; Cangelosi and Meschke, 2014; Carini et al., 2016; Torti et al.,
332 2018; Bradley et al., 2019). Taxonomic identification by molecular methods such as sequencing of
333 the 16S rRNA gene cannot distinguish between active and dormant cells, nor whether the cell is
334 alive or dead (Cangelosi and Meschke, 2014). Indeed, it has been reported that in coastal marine
335 sediments dead cells account for 70 % of all bacterial cells, while among living bacterial cells
336 only 4 % grow actively (Luna et al., 2002). Functional redundancy in microbial communities,
337 which allows functional continuity to be maintained despite changes in composition (Louca et al.,
338 2018), may also allow for some degree of compositional stability despite changing environmental
339 conditions. Indeed, a decoupling of microbial composition and biogeochemical processes has been
340 observed in sediments. Bowen et al. (2011) have shown that microbial communities in sediments
341 are able to resist compositional changes despite significant variations in external nutrient supply,
342 while Marshall et al. (2021) found that the composition of the nitrogen cycling community might
343 change but these compositional changes are not reflected in functional changes. Hence, there is
344 phylogenetic variability realized while there is functional stability.

345 The archaeal community in the Bay of Saline was comprised of *Nanoarchaeota*,
346 *Thermoplasmatota*, *Crenarchaeota* and *Asgardarchaeota* which are all typical sediment members
347 (Zheng et al., 2019; Sun et al., 2020). We found a nearly threefold increase in the relative
348 abundance of *Archaea* in the deepest sediment layer compared to the top layer (Figure 5). This is
349 not surprising as it has been well documented that *Bacteria* dominate the upper sediment layers
350 while at deeper layers the distribution between *Bacteria* and *Archaea* is more uniform (Chen et

351 al., 2017). A particularly pronounced increase in relative abundance with depth was observed for
352 *Thermoplasmatota*. It is possible that oxygen penetration in the uppermost sediment layer caused
353 such a pronounced change as representatives of the Marine Benthic Group D and DHVEG-1,
354 accounting for the majority of sequences within the phylum *Thermoplasmatota* (Rinke et al., 2019),
355 are known to be restricted to anoxic environments (Lloyd et al., 2013).

356 The main difference between the archaeal community of the vegetated and nonvegetated
357 site was the increased presence of *Crenarchaeota* in the nonvegetated sediment (Figure 5). This
358 difference resulted from a much greater increase in the relative abundance of *Bathyarcheia* with
359 increasing depth in the nonvegetated site (Figure 5). In a study comparing archaeal communities
360 in the sediment of a *Zostera marina* meadow with those of bare sediment, a higher presence of
361 *Bathyarchaeota* was found in the vegetated sediment, which is not consistent with our results
362 (Zheng et al., 2019). This discrepancy could have been caused by patchiness and different sampling
363 strategies. In contrast to the three samples per vegetated and nonvegetated sediment in the study of
364 Zheng et al. (2019), we analysed sixty-eight samples from each site. *Bathyarcheia*, formerly known
365 as the Miscellaneous Crenarchaeotal Group (MCG), are typically present in deeper sediment layers
366 as they are well adapted to energy limitation (Kubo et al., 2012). Since seagrasses are known to
367 directly and indirectly enrich the underlying sediment with organic matter (Terrados and Duarte,
368 2000; Duarte, 2002; Duarte et al., 2005; Jensen et al., 2007; van Katwijk et al., 2010; Liu et al.,
369 2017), it is possible that the presence of *C. nodosa* caused the observed lower relative abundance of
370 this group in the sediment at the vegetated site.

371 The sediment bacterial community in the Bay of Saline consisted of taxonomic groups
372 commonly found in marine sediments such as *Desulfobacterota*, *Gammaproteobacteria*,
373 *Bacteroidota*, *Chloroflexi*, and *Planctomycetota* (Walsh et al., 2016; Hoshino et al., 2020), along
374 with *Campylobacterota*, characteristic of seagrass meadows (Jensen et al., 2007). These major
375 groups showed different patterns in relative abundance depending on sediment depth (Figures
376 6 and 7). The proportion of *Gammaproteobacteria* and *Bacteroidota* decreased with sediment

depth, while the relative abundance of *Chloroflexi* increased (Figure 6). Although the proportion of *Desulfobacterota* remained similar in all sediment layers, *Desulfocapsaceae*, a major constituent of the *Desulfobacterota* community, decreased with sediment depth (Figure 6). *Gammaproteobacteria* and *Desulfobacterota* (formerly known as *Deltaproteobacteria*), were reported to decrease with sediment depth, while *Chloroflexi* increased (Petro et al., 2017). Also, Smith et al. (2004) documented no vertical trend in sulphate-reducing prokaryotes (*Desulfobacterota*) over a similarly small depth range. Reduction of sulphate is one of many processes that affects pH in sediments, while oxygen penetration controls the depth of pH minima (Silburn et al., 2017). Because *Desulfocapsaceae* are neutrophilic (Galushko and Kuever, 2021) it is possible that depletion of oxygen below the first centimetre and an increase in hydrogen sulphide with sediment depth (Najdek et al., 2020) contributed to the observed vertical trend of this group. The pronounced decline in *Gammaproteobacteria* after the top centimetre could also be attributed to the oxygen penetration depth observed in the Bay of Saline (Najdek et al., 2020) coinciding with the abrupt change in the relative abundance of this class. Oxygen availability could also influence the vertical distribution of *Chloroflexi* and *Planctomycetota* (Figure 7), as these phyla are known to be prevalent in anoxic sediments (Hoshino et al., 2020). In addition to oxygen availability, the decline of *Gammaproteobacteria* and *Bacteroidota* with sediment depth may also be related to the lower availability of fresh organic matter in deeper layers (Middelburg, 1989), as both of these groups are known to break down and assimilate fresh detritus in coastal sediments (Gihring et al., 2009).

The differences in taxonomic composition of microbial communities from the vegetated and nonvegetated sediment were not as pronounced as those influenced by sediment depth. *Gammaproteobacteria* made up a large proportion of the microbial community in the nonvegetated sediment, and as with vertical structuring, their higher presence at this site could be explained by oxygen availability. This class contains representatives with a wide range of metabolisms, including aerobic species (Gutierrez, 2019), which could benefit from the higher oxygen availability in the nonvegetated sediment (Najdek et al., 2020). Indeed, a study by Ettinger et al. (2017) also found a higher presence of *Gammaproteobacteria* in the sediment outside a seagrass meadow. The

most pronounced difference in the taxonomic composition of this class between the vegetated and nonvegetated site is the higher relative abundance of *Thioalkalspiraceae* in the nonvegetated sediment (Figure 6). This higher relative abundance could be due to differences in organic matter content. In fact, *Thioalkalspiraceae* are known to be chemolithoautotrophs (Mori et al., 2011; Mori and Suzuki, 2014) and thus may rely on inorganic compounds rather than organic matter supplied by the seagrass. Slight differences were also observed in the *Desulfobacterota* community between the vegetated and nonvegetated site. *Desulfosarcinaceae* were more pronounced in the vegetated sediment, while *Desulfobulbaceae* were more pronounced in the nonvegetated sediment (Figure 6). This is consistent with previous studies that reported a high presence of *Desulfosarcinaceae* in vegetated sediments and higher relative abundances of *Desulfobulbaceae* in the nonvegetated sediment (Smith et al., 2004; García-Martínez et al., 2009). Although both families have been associated with the rhizosphere of seagrasses (Cúcio et al., 2016), the high metabolic versatility of *Desulfosarcinaceae* (Watanabe et al., 2020), the most abundant *Desulfobacterota* family in our samples, becomes even more abundant in the vegetated sediment (Figure 6), where high concentrations of different carbon substrates may become available during decomposition of organic matter allowing the proliferation of this group. In contrast to *Gammaproteobacteria* and *Desulfobacterota*, a higher relative abundance of *Bacteroidota* in the vegetated sediment may be influenced by the presence of the plant itself. Seagrass cell walls contain polysaccharides like cellulose (Pfeifer and Classen, 2020) and *Bacteroidota* have been identified as decomposers of macromolecules such as cellulose (Thomas et al., 2011). The differences between the vegetated and nonvegetated sediment communities were also reflected in the higher proportion of *Campylobacterota* related sequences at the vegetated site. *Campylobacterota*, formerly known as *Epsilonproteobacteria*, are known to be closely associated with roots and rhizomes of seagrasses, particularly *Sulfurimonadaceae* (Jensen et al., 2007). In this study, the family *Sulfurimonadaceae* also contributed highly to *Campylobacterota* in the vegetated sediment, possibly due to the proximity of *C. nodosa* roots and rhizomes (Figure 7).

Taken together, sediment microbial communities in the Bay of Saline were depth stratified,

⁴³¹ and differed between the vegetated and nonvegetated site, however, remained temporally stable.
⁴³² Although the *C. nodosa* meadow experienced a sharp decline during the investigation period, no
⁴³³ pronounced change in the microbial community was observed. The characterization of the sediment
⁴³⁴ microbial community of the declining *C. nodosa* meadow in the Bay of Saline forms the basis for
⁴³⁵ further studies based on methods that can differentiate active communities or methods that can
⁴³⁶ provide insight into the prevailing metabolic processes during the period of seagrass decline.

437 **Acknowledgements**

438 This study was funded by the Croatian Science Foundation through the MICRO-SEAGRASS
439 project (project number IP-2016-06-7118). GJH was supported by the Austrian Science Fund
440 (FWF) through the ARTEMIS project (project number P28781-B21). We would like to thank the
441 University Computing Center of the University of Zagreb for access to the computer cluster Isabella,
442 Margareta Buterer for technical support and Paolo Paliaga for help during sampling.

443 **References**

- 444 Allaire, J. J., Xie, Y., McPherson, J., Luraschi, J., Ushey, K., Atkins, A., et al. (2021).
- 445 *rmarkdown: Dynamic documents for R.*
- 446 Apprill, A., McNally, S., Parsons, R., and Weber, L. (2015). Minor revision to V4 region SSU
- 447 rRNA 806R gene primer greatly increases detection of SAR11 bacterioplankton. *Aquat. Microb. Ecol.* 75, 129–137. doi:10.3354/ame01753.
- 449 Bent, S. J., and Forney, L. J. (2008). The tragedy of the uncommon: Understanding limitations
- 450 in the analysis of microbial diversity. *ISME J.* 2, 689–695. doi:10.1038/ismej.2008.44.
- 451 Borcard, D., Gillet, F., and Legendre, P. (2018). *Numerical ecology with R*. 2nd ed. New York:
- 452 Springer-Verlag doi:10.1007/978-3-319-71404-2.
- 453 Bourque, A. S., Vega-Thurber, R., and Fourqurean, J. W. (2015). Microbial community
- 454 structure and dynamics in restored subtropical seagrass sediments. *Aquat. Microb. Ecol.* 74, 43–57.
- 455 doi:10.3354/ame01725.
- 456 Bowen, J. L., Ward, B. B., Morrison, H. G., Hobbie, J. E., Valiela, I., Deegan, L. A., et al.
- 457 (2011). Microbial community composition in sediments resists perturbation by nutrient enrichment.
- 458 *ISME J.* 5, 1540–1548. doi:10.1038/ismej.2011.22.
- 459 Bradley, J. A., Amend, J. P., and LaRowe, D. E. (2019). Survival of the fewest: Microbial
- 460 dormancy and maintenance in marine sediments through deep time. *Geobiology* 17, 43–59.
- 461 doi:10.1111/gbi.12313.
- 462 Cangelosi, G. A., and Meschke, J. S. (2014). Dead or alive: Molecular assessment of microbial
- 463 viability. *Appl. Environ. Microbiol.* 80, 5884–5891. doi:10.1128/AEM.01763-14.

464 Caporaso, J. G., Lauber, C. L., Walters, W. A., Berg-Lyons, D., Huntley, J., Fierer, N., et al.
465 (2012). Ultra-high-throughput microbial community analysis on the Illumina HiSeq and MiSeq
466 platforms. *ISME J.* 6, 1621–1624. doi:10.1038/ismej.2012.8.

467 Caporaso, J. G., Lauber, C. L., Walters, W. A., Berg-Lyons, D., Lozupone, C. A., Turnbaugh,
468 P. J., et al. (2011). Global patterns of 16S rRNA diversity at a depth of millions of sequences per
469 sample. *Proc. Natl. Acad. Sci. U.S.A.* 108, 4516–4522. doi:10.1073/pnas.1000080107.

470 Carini, P., Marsden, P. J., Leff, J. W., Morgan, E. E., Strickland, M. S., and Fierer, N. (2016).
471 Relic DNA is abundant in soil and obscures estimates of soil microbial diversity. *Nat. Microbiol.* 2,
472 16242. doi:10.1038/nmicrobiol.2016.242.

473 Chen, X., Andersen, T. J., Morono, Y., Inagaki, F., Jørgensen, B. B., and Lever, M. A. (2017).
474 Bioturbation as a key driver behind the dominance of bacteria over archaea in near-surface sediment.
475 *Sci. Rep.* 7, 2400. doi:10.1038/s41598-017-02295-x.

476 Cúcio, C., Engelen, A. H., Costa, R., and Muyzer, G. (2016). Rhizosphere microbiomes of
477 european seagrasses are selected by the plant, but are not species specific. *Front. Microbiol.* 7, 440.
478 doi:10.3389/fmicb.2016.00440.

479 Duarte, C. (2002). The future of seagrass meadows. *Environ. Conserv.* 29, 192–206.
480 doi:10.1017/S0376892902000127.

481 Duarte, C. M., Holmer, M., and Marbà, N. (2005). “Plant microbe interactions in seagrass
482 meadows,” in *Interactions between macro- and microorganisms in marine sediments*, eds. E.
483 Kristensen, R. R. Haese, and J. E. Kostka (Washington: American Geophysical Union), 31–60.
484 doi:10.1029/CE060p0031.

485 Edwards, M. S. (2020). *lemon: Freshing up your 'ggplot2' plots.*

- 486 Ettinger, C. L., Voerman, S. E., Lang, J. M., Stachowicz, J. J., and Eisen, J. A. (2017).
- 487 Microbial communities in sediment from *Zostera marina* patches, but not the *Z. marina* leaf or root
- 488 microbiomes, vary in relation to distance from patch edge. *PeerJ* 5, e3246. doi:10.7717/peerj.3246.
- 489 Fonseca, M. S., and Kenworthy, W. J. (1987). Effects of current on photosynthesis and
- 490 distribution of seagrasses. *Aquat. Bot.* 27, 59–78. doi:10.1016/0304-3770(87)90086-6.
- 491 Galushko, A., and Kuever, J. (2021). “*Desulfocapsaceae*,” in *Bergey’s manual of systematics*
- 492 *of Archaea and Bacteria*, ed. W. B. Whitman (online: John Wiley & Sons, in association with
- 493 Bergey’s manual trust), 1–6. doi:10.1002/9781118960608.fbm00332.
- 494 García-Martínez, M., López-López, A., Calleja, M. L., Marbà, N., and Duarte, C. M. (2009).
- 495 Bacterial community dynamics in a seagrass (*Posidonia oceanica*) meadow sediment. *Estuaries*
- 496 *Coasts* 32, 276–286. doi:10.1007/s12237-008-9115-y.
- 497 Gihring, T. M., Humphrys, M., Mills, H. J., Huette, M., and Kostka, J. E. (2009). Identification
- 498 of phytodetritus-degrading microbial communities in sublittoral Gulf of Mexico sands. *Limnol.*
- 499 *Oceanogr.* 54, 1073–1083. doi:10.4319/lo.2009.54.4.1073.
- 500 Guevara, R., Ikenaga, M., Dean, A. L., Pisani, C., and Boyer, J. N. (2014). Changes in
- 501 sediment bacterial community in response to long-term nutrient enrichment in a subtropical
- 502 seagrass-dominated estuary. *Microb. Ecol.* 68, 427–440. doi:10.1007/s00248-014-0418-1.
- 503 Gutierrez, T. (2019). “Marine, aerobic hydrocarbon-degrading *Gammaproteobacteria*:
- 504 Overview,” in *Taxonomy, genomics and ecophysiology of hydrocarbon-degrading microbes*, ed. T. J.
- 505 McGenity (Cham: Springer-Verlag), 143–152. doi:10.1007/978-3-030-14796-9_22.
- 506 Hamdan, L. J., Coffin, R. B., Sikaroodi, M., Greinert, J., Treude, T., and Gillevet, P. M.
- 507 (2013). Ocean currents shape the microbiome of Arctic marine sediments. *ISME J.* 7, 685–696.
- 508 doi:10.1038/ismej.2012.143.

- 509 Hoshino, T., Doi, H., Uramoto, G.-I., Wörmer, L., Adhikari, R. R., Xiao, N., et al. (2020).
510 Global diversity of microbial communities in marine sediment. *Proc. Natl. Acad. Sci. U.S.A.* 117,
511 27587–27597. doi:10.1073/pnas.1919139117.
- 512 Jensen, S. I., Kühl, M., and Priemé, A. (2007). Different bacterial communities associated with
513 the roots and bulk sediment of the seagrass *Zostera marina*. *FEMS Microbiol. Ecol.* 62, 108–117.
514 doi:10.1111/j.1574-6941.2007.00373.x.
- 515 Jones, S. E., and Lennon, J. T. (2010). Dormancy contributes to the maintenance of microbial
516 diversity. *Proc. Natl. Acad. Sci. U.S.A.* 107, 5881–5886. doi:10.1073/pnas.0912765107.
- 517 Jost, L. (2006). Entropy and diversity. *Oikos* 113, 363–375.
518 doi:10.1111/j.2006.0030-1299.14714.x.
- 519 Jørgensen, B. B., and Marshall, I. P. (2016). Slow microbial life in the seabed. *Annu. Rev. Mar.*
520 *Sci.* 8, 311–332. doi:10.1146/annurev-marine-010814-015535.
- 521 Kirkpatrick, J. B., Walsh, E. A., and D’Hondt, S. (2019). Microbial selection and survival in
522 subseafloor sediment. *Front. Microbiol.* 10, 956. doi:10.3389/fmicb.2019.00956.
- 523 Korlević, M., Markovski, M., Zhao, Z., Herndl, G. J., and Najdek, M. (2021a). Seasonal
524 dynamics of epiphytic microbial communities on marine macrophyte surfaces. *Front. Microbiol.*
525 12, 2528. doi:10.3389/fmicb.2021.671342.
- 526 Korlević, M., Markovski, M., Zhao, Z., Herndl, G. J., and Najdek, M. (2021b). Selective
527 DNA and protein isolation from marine macrophyte surfaces. *Front. Microbiol.* 12, 665999.
528 doi:10.3389/fmicb.2021.665999.

- 529 Kozich, J. J., Westcott, S. L., Baxter, N. T., Highlander, S. K., and Schloss, P. D. (2013).
530 Development of a dual-index sequencing strategy and curation pipeline for analyzing amplicon
531 sequence data on the MiSeq Illumina sequencing platform. *Appl. Environ. Microbiol.* 79,
532 5112–5120. doi:10.1128/AEM.01043-13.
- 533 Kubo, K., Lloyd, K. G., F Biddle, J., Amann, R., Teske, A., and Knittel, K. (2012). *Archaea* of
534 the Miscellaneous Crenarchaeotal Group are abundant, diverse and widespread in marine sediments.
535 *ISME J.* 6, 1949–1965. doi:10.1038/ismej.2012.37.
- 536 Legendre, P., and Legendre, L. (2012). *Numerical ecology*. 3rd ed. Amsterdam: Elsevier.
- 537 Liu, S., Jiang, Z., Deng, Y., Wu, Y., Zhao, C., Zhang, J., et al. (2017). Effects of seagrass leaf
538 litter decomposition on sediment organic carbon composition and the key transformation processes.
539 *Sci. China Earth Sci.* 60, 2108–2117. doi:10.1007/s11430-017-9147-4.
- 540 Lloyd, K. G., Schreiber, L., Petersen, D. G., Kjeldsen, K. U., Lever, M. A., Steen, A. D., et al.
541 (2013). Predominant archaea in marine sediments degrade detrital proteins. *Nature* 496, 215–218.
542 doi:10.1038/nature12033.
- 543 Louca, S., Polz, M. F., Mazel, F., Albright, M. B. N., Huber, J. A., O'Connor, M. I., et al.
544 (2018). Function and functional redundancy in microbial systems. *Nat. Ecol. Evol.* 2, 936–943.
545 doi:10.1038/s41559-018-0519-1.
- 546 Luna, G. M., Manini, E., and Danovaro, R. (2002). Large fraction of dead and inactive bacteria
547 in coastal marine sediments: Comparison of protocols for determination and ecological significance.
548 *Appl. Environ. Microbiol.* 68, 3509–3513. doi:10.1128/AEM.68.7.3509-3513.2002.
- 549 Marshall, A., Longmore, A., Phillips, L., Tang, C., Hayden, H., Heidelberg, K., et al. (2021).
550 Nitrogen cycling in coastal sediment microbial communities with seasonally variable benthic
551 nutrient fluxes. *Aquat. Microb. Ecol.* 86, 1–19. doi:10.3354/ame01954.

- 552 Marshall, I. P. G., Ren, G., Jaussi, M., Lomstein, B. A., Jørgensen, B. B., Røy, H., et al. (2019).
553 Environmental filtering determines family-level structure of sulfate-reducing microbial communities
554 in subsurface marine sediments. *ISME J.* 13, 1920–1932. doi:10.1038/s41396-019-0387-y.
- 555 Middelburg, J. J. (1989). A simple rate model for organic matter decomposition in marine
556 sediments. *Geochim. Cosmochim. Acta* 53, 1577–1581. doi:10.1016/0016-7037(89)90239-1.
- 557 Mori, K., and Suzuki, K.-i. (2014). “The family *Thioalkalispiraceae*,” in *The prokaryotes: Gammaproteobacteria*, eds. E. Rosenberg, E. F. DeLong, S. Lory, E. Stackebrandt, and F. Thompson (Berlin, Heidelberg: Springer-Verlag), 653–658. doi:10.1007/978-3-642-38922-1_399.
- 560 Mori, K., Suzuki, K.-I., Urabe, T., Sugihara, M., Tanaka, K., Hamada, M., et al. (2011).
561 *Thiopropfundum hispidum* sp. nov., an obligately chemolithoautotrophic sulfur-oxidizing
562 gammaproteobacterium isolated from the hydrothermal field on Suiyo Seamount, and proposal
563 of *Thioalkalispiraceae* fam. nov. in the order *Chromatiales*. *Int. J. Syst. Evol. Microbiol.* 61,
564 2412–2418. doi:10.1099/ijts.0.026963-0.
- 565 Najdek, M., Korlević, M., Paliaga, P., Markovski, M., Ivančić, I., Iveša, L., et al. (2020).
566 Dynamics of environmental conditions during the decline of a *Cymodocea nodosa* meadow.
567 *Biogeosciences* 17, 3299–3315. doi:10.5194/bg-17-3299-2020.
- 568 Neuwirth, E. (2014). *RColorBrewer: ColorBrewer palettes*.
- 569 Oksanen, J., Blanchet, F. G., Friendly, M., Kindt, R., Legendre, P., McGlinn, D., et al. (2020).
570 *vegan: Community ecology package*.
- 571 Orcutt, B. N., Sylvan, J. B., Knab, N. J., and Edwards, K. J. (2011). Microbial ecology
572 of the dark ocean above, at, and below the seafloor. *Microbiol. Mol. Biol. Rev.* 75, 361–422.
573 doi:10.1128/MMBR.00039-10.

- 574 Orlando-Bonaca, M., Francé, J., Mavrič, B., Grego, M., Lipej, L., Flander-Putrl, V., et al.
575 (2015). A new index (MediSkew) for the assessment of the *Cymodocea nodosa* (Ucria) Ascherson
576 meadow's status. *Mar. Environ. Res.* 110, 132–141. doi:10.1016/j.marenvres.2015.08.009.
- 577 Orsi, W. D. (2018). Ecology and evolution of seafloor and subseafloor microbial communities.
578 *Nat. Rev. Microbiol.* 16, 671–683. doi:10.1038/s41579-018-0046-8.
- 579 Parada, A. E., Needham, D. M., and Fuhrman, J. A. (2016). Every base matters: Assessing
580 small subunit rRNA primers for marine microbiomes with mock communities, time series and
581 global field samples. *Environ. Microbiol.* 18, 1403–1414. doi:10.1111/1462-2920.13023.
- 582 Petro, C., Starnawski, P., Schramm, A., and Kjeldsen, K. (2017). Microbial community
583 assembly in marine sediments. *Aquat. Microb. Ecol.* 79, 177–195. doi:10.3354/ame01826.
- 584 Petro, C., Zäncker, B., Starnawski, P., Jochum, L. M., Ferdelman, T. G., Jørgensen, B. B., et
585 al. (2019). Marine deep biosphere microbial communities assemble in near-surface sediments in
586 Aarhus Bay. *Front. Microbiol.* 10, 758. doi:10.3389/fmicb.2019.00758.
- 587 Pfeifer, L., and Classen, B. (2020). The cell wall of seagrasses: Fascinating, peculiar and a
588 blank canvas for future research. *Front. Plant Sci.* 11, 588754. doi:10.3389/fpls.2020.588754.
- 589 Pjevac, P., Meier, D. V., Markert, S., Hentschker, C., Schweder, T., Becher, D., et al. (2018).
590 Metaproteogenomic profiling of microbial communities colonizing actively venting hydrothermal
591 chimneys. *Front. Microbiol.* 9, 680. doi:10.3389/fmicb.2018.00680.
- 592 Polymenakou, P., Bertilsson, S., Tselepidis, A., and Stephanou, E. (2005). Bacterial
593 community composition in different sediments from the Eastern Mediterranean Sea: A
594 comparison of four 16S ribosomal DNA clone libraries. *Microb. Ecol.* 50, 447–62.
595 doi:10.1007/s00248-005-0005-6.

596 Quast, C., Pruesse, E., Yilmaz, P., Gerken, J., Schweer, T., Yarza, P., et al. (2013). The SILVA
597 ribosomal RNA gene database project: Improved data processing and web-based tools. *Nucleic*
598 *Acids Res.* 41, D590–D596. doi:10.1093/nar/gks1219.

599 Rabbani, G., Yan, B. C., Lee, N. L. Y., Ooi, J. L. S., Lee, J. N., Huang, D., et al. (2021). Spatial
600 and structural factors shape seagrass-associated bacterial communities in Singapore and Peninsular
601 Malaysia. *Front. Mar. Sci.* 8, 590. doi:10.3389/fmars.2021.659180.

602 R Core Team (2020). *R: A language and environment for statistical computing*. Vienna,
603 Austria: R foundation for statistical computing.

604 Rinke, C., Rubino, F., Messer, L. F., Youssef, N., Parks, D. H., Chuvochina, M., et al. (2019).
605 A phylogenomic and ecological analysis of the globally abundant Marine Group II archaea (*Ca.*
606 *Poseidoniales* ord. nov.). *ISME J.* 13, 663–675. doi:10.1038/s41396-018-0282-y.

607 Ruiz Fernandez, J. M., Boudouresque, C., and Enríquez, S. (2009). Seagrass ecosystems and
608 Mediterranean seagrasses. *Botanica Marina* 52, 369–381. doi:10.1515/BOT.2009.058.

609 Schloss, P. D., Jenior, M. L., Koumpouras, C. C., Westcott, S. L., and Highlander, S. K. (2016).
610 Sequencing 16S rRNA gene fragments using the PacBio SMRT DNA sequencing system. *PeerJ* 4,
611 e1869. doi:10.7717/peerj.1869.

612 Schloss, P. D., Westcott, S. L., Ryabin, T., Hall, J. R., Hartmann, M., Hollister, E. B., et al.
613 (2009). Introducing mothur: Open-source, platform-independent, community-supported software
614 for describing and comparing microbial communities. *Appl. Environ. Microbiol.* 75, 7537–7541.
615 doi:10.1128/AEM.01541-09.

616 Silburn, B., Kröger, S., Parker, E. R., Sivyer, D. B., Hicks, N., Powell, C. F., et al. (2017).
617 Benthic pH gradients across a range of shelf sea sediment types linked to sediment characteristics
618 and seasonal variability. *Biogeochemistry* 135, 69–88. doi:10.1007/s10533-017-0323-z.

- 619 Smith, A. C., Kostka, J. E., Devereux, R., and Yates, D. F. (2004). Seasonal composition and
620 activity of sulfate-reducing prokaryotic communities in seagrass bed sediments. *Aquat. Microb.*
621 *Ecol.* 37, 183–195. doi:10.3354/ame037183.
- 622 Starnawski, P., Bataillon, T., Ettema, T. J. G., Jochum, L. M., Schreiber, L., Chen, X., et al.
623 (2017). Microbial community assembly and evolution in subseafloor sediment. *Proc. Natl. Acad.*
624 *Sci. U.S.A.* 114, 2940–2945. doi:10.1073/pnas.1614190114.
- 625 Sun, F., Zhang, X., Zhang, Q., Liu, F., Zhang, J., and Gong, J. (2015). Seagrass (*Zostera*
626 *marina*) colonization promotes the accumulation of diazotrophic bacteria and alters the relative
627 abundances of specific bacterial lineages involved in benthic carbon and sulfur cycling. *Appl.*
628 *Environ. Microbiol.* 81, 6901–6914. doi:10.1128/AEM.01382-15.
- 629 Sun, Y., Song, Z., Zhang, H., Liu, P., and Hu, X. (2020). Seagrass vegetation affect the
630 vertical organization of microbial communities in sediment. *Mar. Environ. Res.* 162, 105174.
631 doi:10.1016/j.marenvres.2020.105174.
- 632 Terrados, J., and Duarte, C. M. (2000). Experimental evidence of reduced particle
633 resuspension within a seagrass (*Posidonia oceanica*) meadow. *J. Exp. Mar. Biol. Ecol.* 243, 45–53.
634 doi:10.1016/S0022-0981(99)00110-0.
- 635 Thomas, F., Hehemann, J.-H., Rebuffet, E., Czjzek, M., and Michel, G. (2011).
636 Environmental and gut *Bacteroidetes*: The food connection. *Front. Microbiol.* 2, 93.
637 doi:10.3389/fmicb.2011.00093.
- 638 Torti, A., Jørgensen, B. B., and Lever, M. A. (2018). Preservation of microbial DNA in
639 marine sediments: Insights from extracellular DNA pools. *Environ. Microbiol.* 20, 4526–4542.
640 doi:10.1111/1462-2920.14401.

- 641 Tuya, F., Ribeiro-Leite, L., Arto-Cuesta, N., Coca, J., Haroun, R., and Espino, F. (2014).
- 642 Decadal changes in the structure of *Cymodocea nodosa* seagrass meadows: Natural vs. human
643 influences. *Estuar. Coast. Shelf Sci.* 137, 41–49. doi:10.1016/j.ecss.2013.11.026.
- 644 van Katwijk, M. M., Bos, A. R., Hermus, D. C. R., and Suykerbuyk, W. (2010). Sediment
645 modification by seagrass beds: Muddification and sandification induced by plant cover and
646 environmental conditions. *Estuar. Coast. Shelf Sci.* 89, 175–181. doi:10.1016/j.ecss.2010.06.008.
- 647 Walsh, E. A., Kirkpatrick, J. B., Rutherford, S. D., Smith, D. C., Sogin, M., and D'Hondt, S.
648 (2016). Bacterial diversity and community composition from seafloor to subseafloor. *ISME J.* 10,
649 979–989. doi:10.1038/ismej.2015.175.
- 650 Watanabe, M., Fukui, M., Galushko, A., and Kuever, J. (2020). “*Desulfosarcina*,” in *Bergey's*
651 *manual of systematics of Archaea and Bacteria*, ed. W. B. Whitman (online: John Wiley & Sons, in
652 association with Bergey's manual trust), 1–6. doi:10.1002/9781118960608.gbm01020.pub2.
- 653 Wickham, H., Averick, M., Bryan, J., Chang, W., McGowan, L. D., François, R., et al. (2019).
- 654 Welcome to the tidyverse. *J. Open Source Softw.* 4, 1686. doi:10.21105/joss.01686.
- 655 Wilke, C. O. (2020). *Cowplot: Streamlined plot theme and plot annotations for 'ggplot2'*.
- 656 Xie, Y. (2014). “knitr: A comprehensive tool for reproducible research in R,” in *Implementing*
657 *reproducible computational research*, eds. V. Stodden, F. Leisch, and R. D. Peng (New York:
658 Chapman and Hall/CRC), 3–32.
- 659 Xie, Y. (2015). *Dynamic documents with R and knitr*. 2nd ed. Boca Raton, Florida: Chapman
660 and Hall/CRC.
- 661 Xie, Y. (2019). TinyTeX: A lightweight, cross-platform, and easy-to-maintain LaTeX
662 distribution based on TeX Live. *TUGboat* 40, 30–32.
- 663 Xie, Y. (2021a). *knitr: A general-purpose package for dynamic report generation in R*.

- 664 Xie, Y. (2021b). *tinytex: Helper functions to install and maintain 'TeX Live', and compile*
665 *'LaTeX' documents.*
- 666 Xie, Y., Allaire, J. J., and Grolemund, G. (2018). *R Markdown: The definitive guide*. 1st ed.
667 Boca Raton, Florida: Chapman and Hall/CRC.
- 668 Xie, Y., Deriveux, C., and Riederer, E. (2020). *R Markdown cookbook*. 1st ed. Boca Raton,
669 Florida: Chapman and Hall/CRC.
- 670 Yilmaz, P., Parfrey, L. W., Yarza, P., Gerken, J., Pruesse, E., Quast, C., et al. (2014). The
671 SILVA and “All-species Living Tree Project (LTP)” taxonomic frameworks. *Nucleic Acids Res.* 42,
672 D643–D648. doi:10.1093/nar/gkt1209.
- 673 Zhang, X., Zhao, C., Yu, S., Jiang, Z., Liu, S., Wu, Y., et al. (2020). Rhizosphere microbial
674 community structure is selected by habitat but not plant species in two tropical seagrass beds. *Front.*
675 *Microbiol.* 11, 161. doi:10.3389/fmicb.2020.00161.
- 676 Zheng, P., Wang, C., Zhang, X., and Gong, J. (2019). Community structure and abundance of
677 archaea in a *Zostera marina* meadow: A comparison between seagrass-colonized and bare sediment
678 sites. *Archaea* 2019, e5108012. doi:10.1155/2019/5108012.
- 679 Zhou, J., Bruns, M. A., and Tiedje, J. M. (1996). DNA recovery from soils of diverse
680 composition. *Appl. Environ. Microbiol.* 62, 316–322. doi:10.1128/aem.62.2.316-322.1996.
- 681 Zhu, H. (2021). *kableExtra: Construct complex table with 'kable' and pipe syntax*.

682 **Figure legends**

683 **Figure 1.** Location of the vegetated (declining *Cymodocea nodosa* meadow) and
684 nonvegetated site in the Bay of Saline, northern Adriatic Sea (© OpenStreetMap contributors,
685 www.openstreetmap.org/copyright).

686 **Figure 2.** The observed number of OTUs, Chao1, ACE, exponential of the Shannon diversity
687 index, and Inverse Simpson diversity index of sediment microbial communities sampled in different
688 sediment layers of the vegetated and nonvegetated site in the Bay of Saline.

689 **Figure 3.** Principal Coordinates Analysis (PCoA) of Bray-Curtis dissimilarities based on OTU
690 abundances of sediment microbial communities sampled in the Bay of Saline. Samples from
691 different sites are labelled with different symbols while samples from different sediment layers
692 are indicated by colour. The proportion of explained variation by each axis is shown on the
693 corresponding axis in parentheses.

694 **Figure 4.** Principal Coordinates Analyses (PCoA) of Bray-Curtis dissimilarities based on OTU
695 abundances of sediment microbial communities, of all and individual sediment layers, sampled at
696 the vegetated and nonvegetated site in the Bay of Saline. The proportion of explained variation by
697 each axis is shown on the corresponding axis in parentheses.

698 **Figure 5.** Taxonomic classification and relative contribution of the most abundant bacterial and
699 archaeal ($\geq 3\%$) sequences in sediment communities sampled at the vegetated and nonvegetated
700 site in the Bay of Saline. NR – sequences without known relatives

701 **Figure 6.** Taxonomic classification and relative contribution of the most abundant ($\geq 2\%$) taxonomic
702 groups within *Desulfobacterota*, *Gammaproteobacteria*, and *Bacteroidota* in sediment communities
703 sampled at the vegetated and nonvegetated site in the Bay of Saline. NR – sequences without known
704 relatives

705 **Figure 7.** Taxonomic classification and relative contribution of the most abundant ($\geq 1\%$) taxonomic
706 groups within *Chloroflexi*, *Planctomycetota*, and *Campylobacterota* in sediment communities
707 sampled at the vegetated and nonvegetated site in the Bay of Saline. NR – sequences without known
708 relatives

709 **Figures**

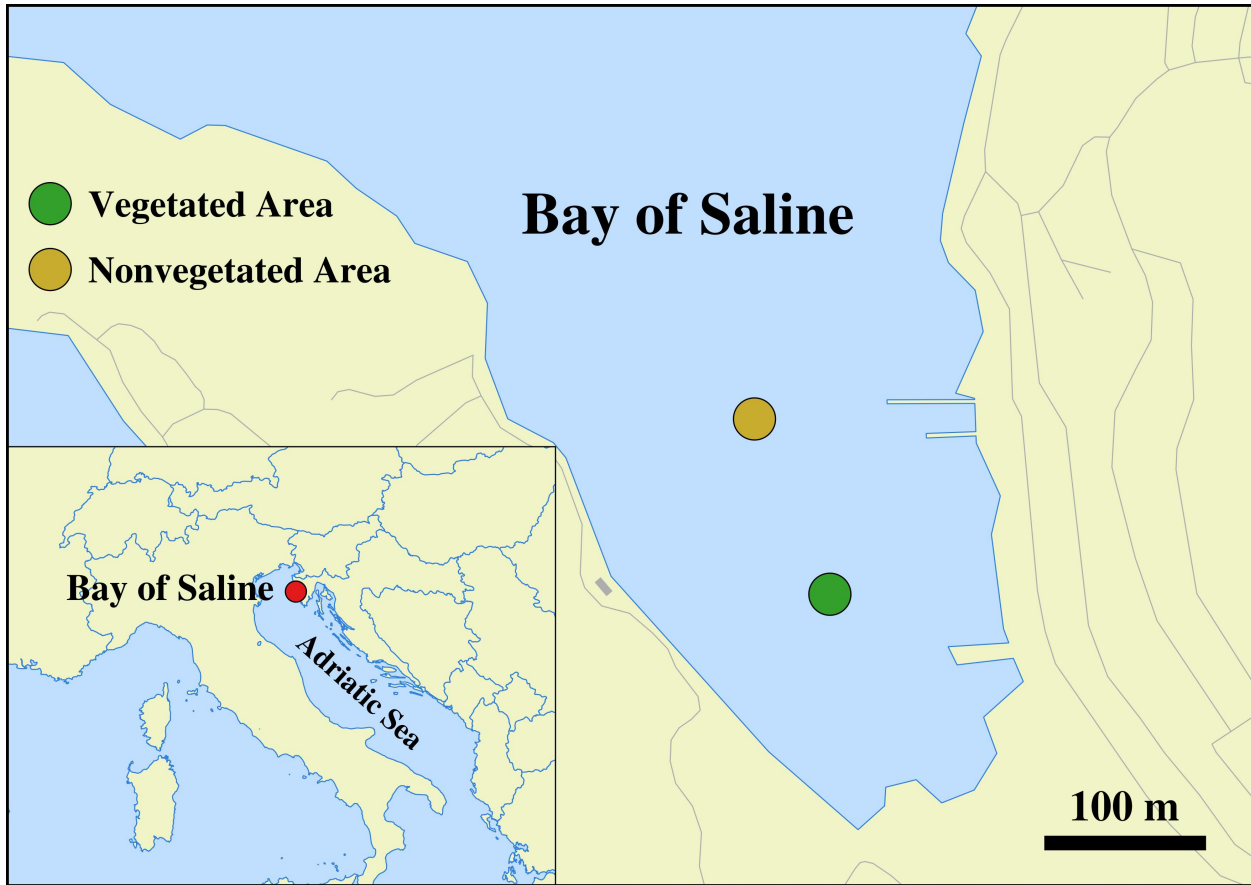


Figure 1. Location of the vegetated (declining *Cymodocea nodosa* meadow) and nonvegetated site in the Bay of Saline, northern Adriatic Sea (© OpenStreetMap contributors, www.openstreetmap.org/copyright).

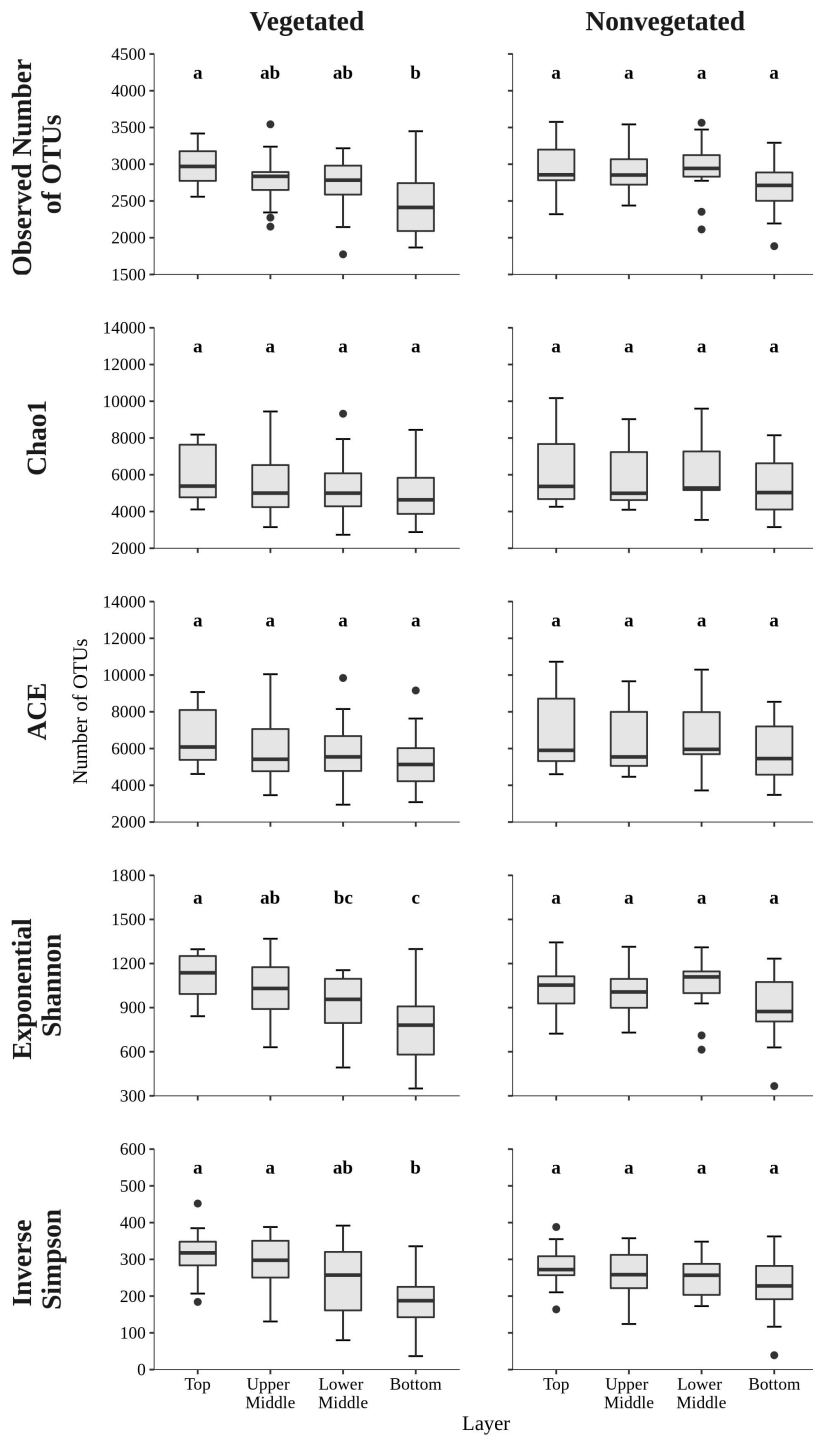


Figure 2. The observed number of OTUs, Chao1, ACE, exponential of the Shannon diversity index, and Inverse Simpson diversity index of sediment microbial communities sampled in different sediment layers of the vegetated and nonvegetated site in the Bay of Saline.

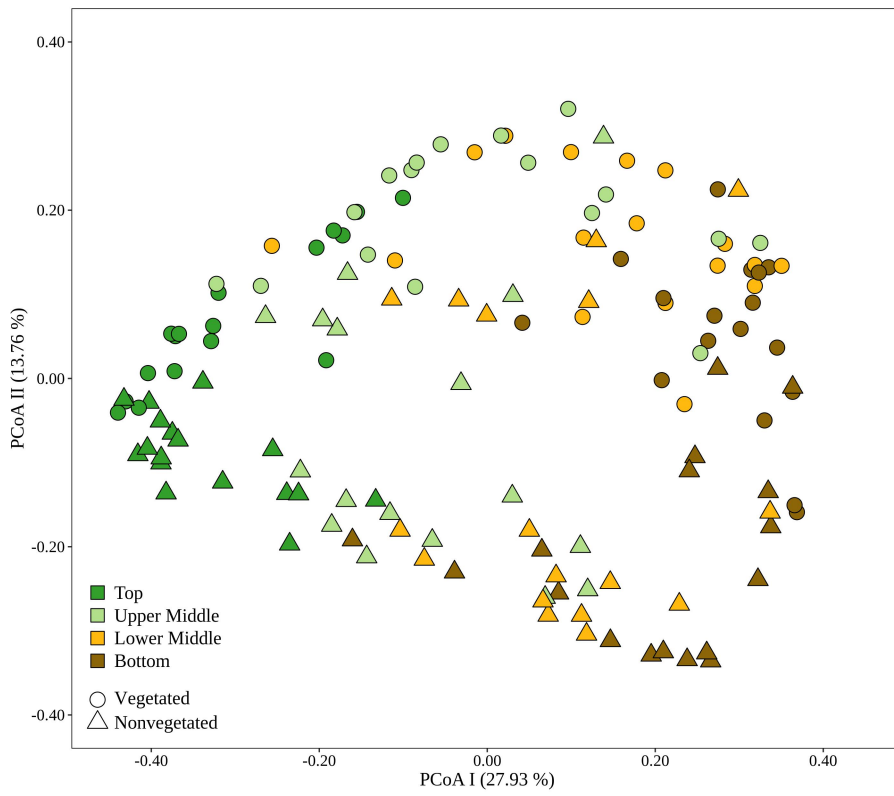


Figure 3. Principal Coordinates Analysis (PCoA) of Bray-Curtis dissimilarities based on OTU abundances of sediment microbial communities sampled in the Bay of Saline. Samples from different sites are labelled with different symbols while samples from different sediment layers are indicated by colour. The proportion of explained variation by each axis is shown on the corresponding axis in parentheses.

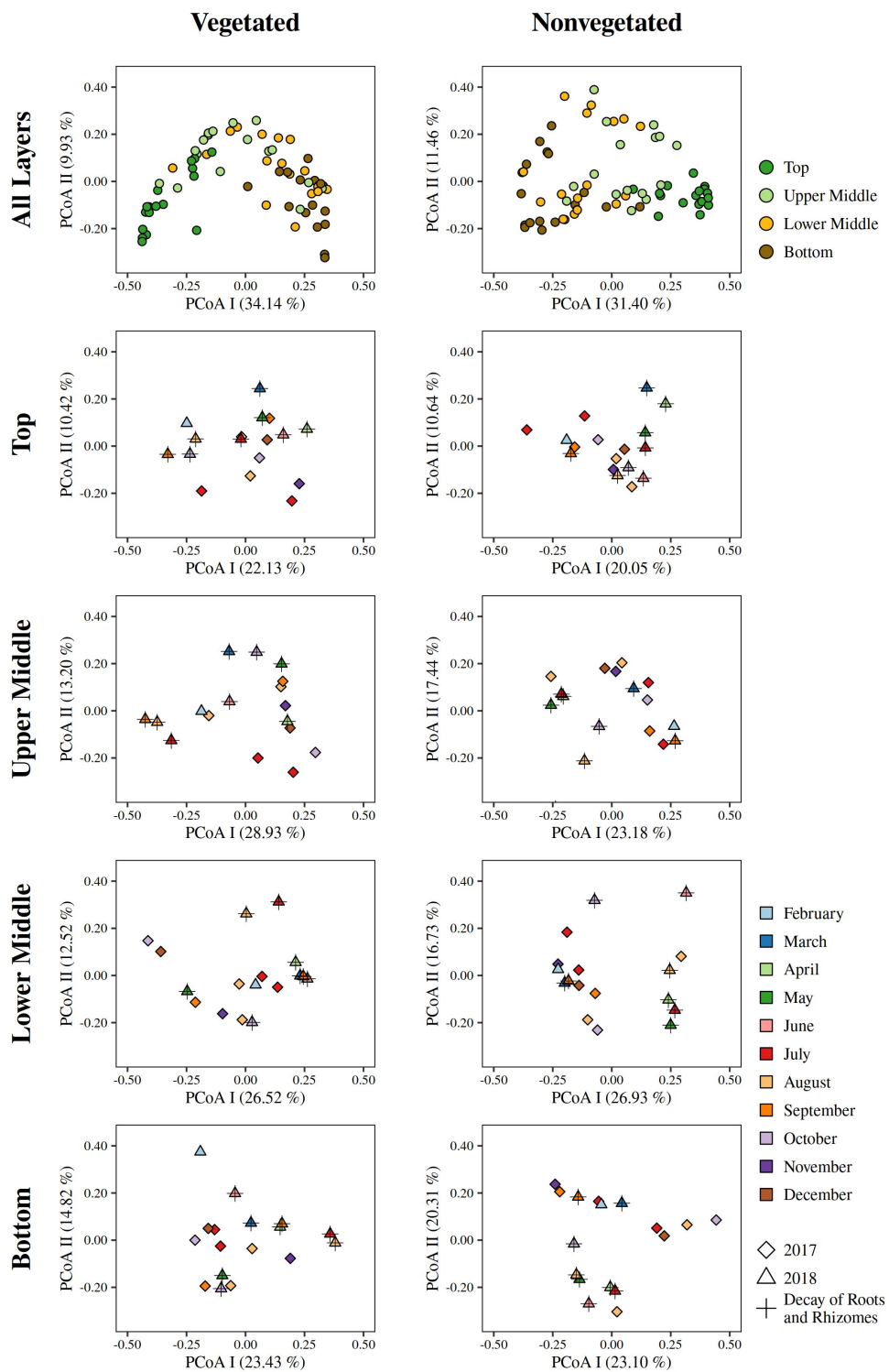


Figure 4. Principal Coordinates Analyses (PCoA) of Bray-Curtis dissimilarities based on OTU abundances of sediment microbial communities, of all and individual sediment layers, sampled at the vegetated and nonvegetated site in the Bay of Saline. The proportion of explained variation by each axis is shown on the corresponding axis in parentheses.

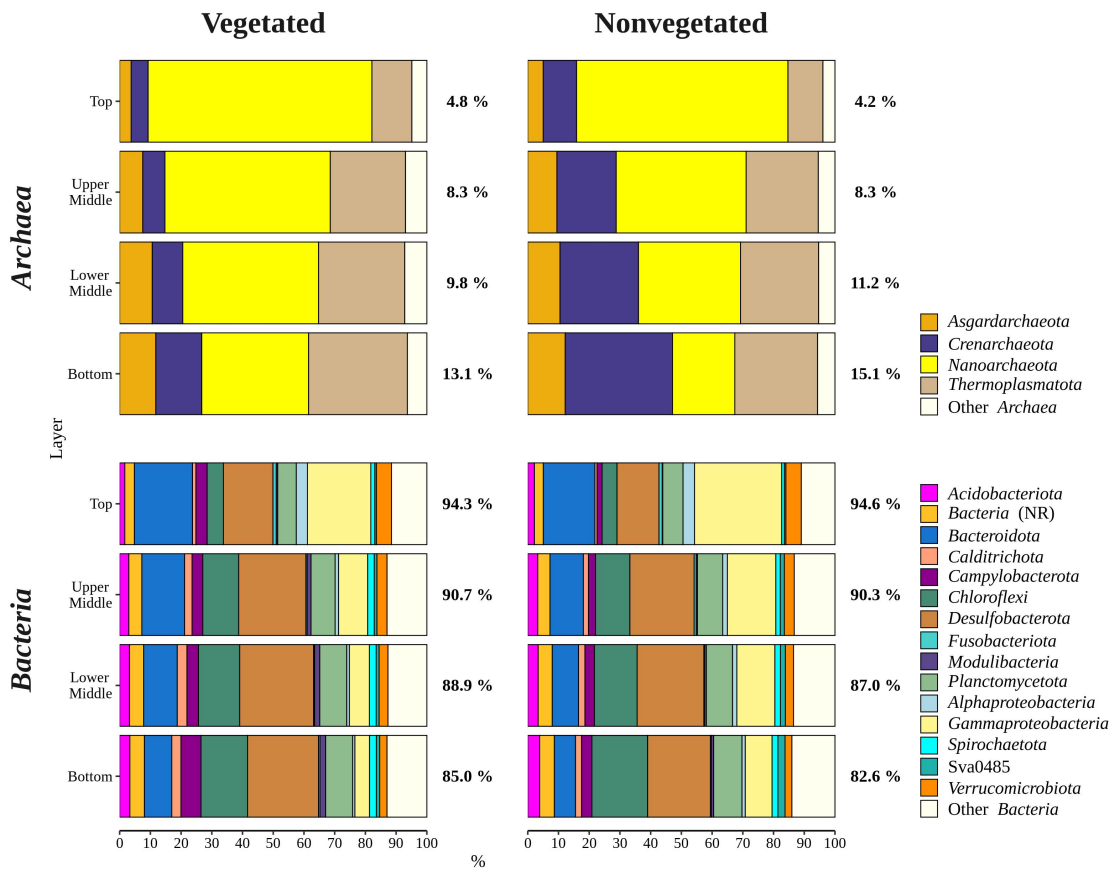


Figure 5. Taxonomic classification and relative contribution of the most abundant bacterial and archaeal ($\geq 3\%$) sequences in sediment communities sampled at the vegetated and nonvegetated site in the Bay of Saline. NR – sequences without known relatives

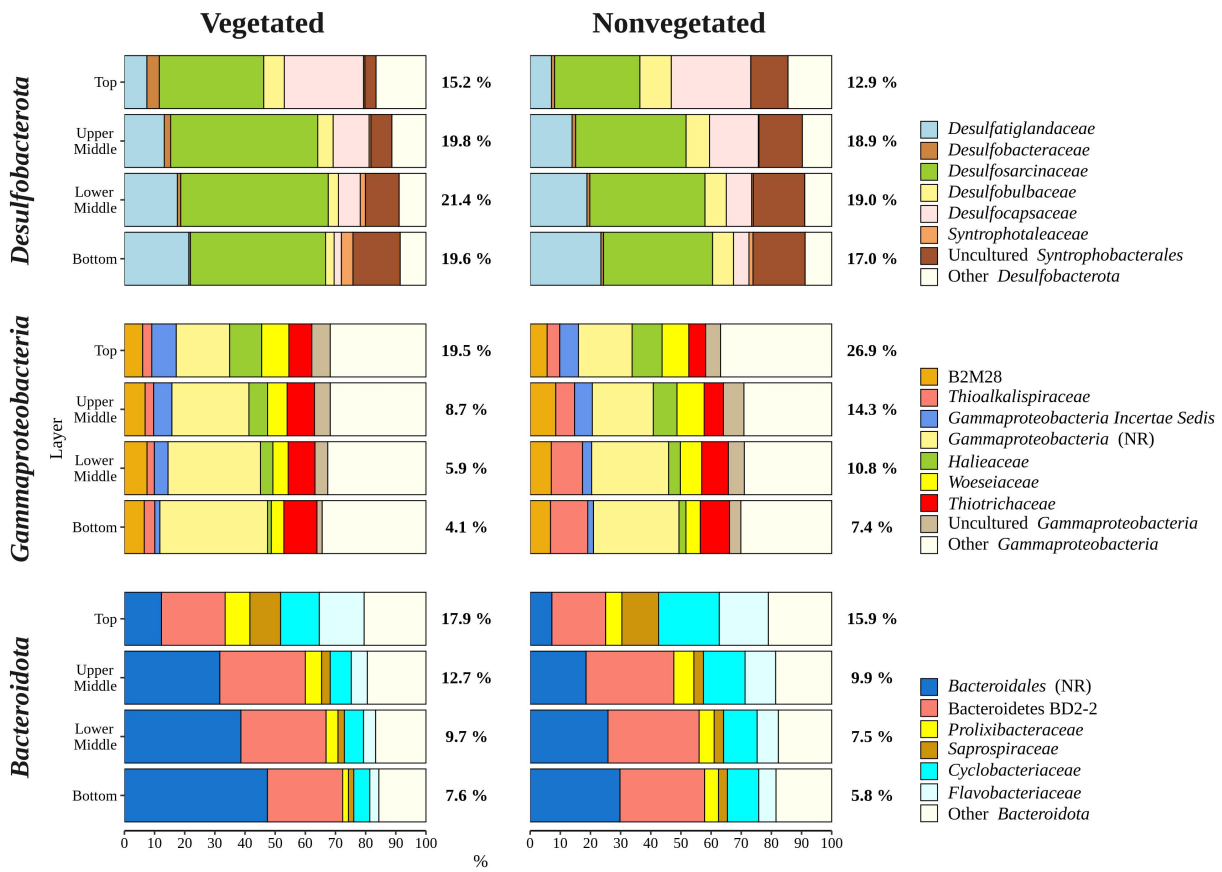


Figure 6. Taxonomic classification and relative contribution of the most abundant ($\geq 2\%$) taxonomic groups within *Desulfobacterota*, *Gammaproteobacteria*, and *Bacteroidota* in sediment communities sampled at the vegetated and nonvegetated site in the Bay of Saline. NR – sequences without known relatives

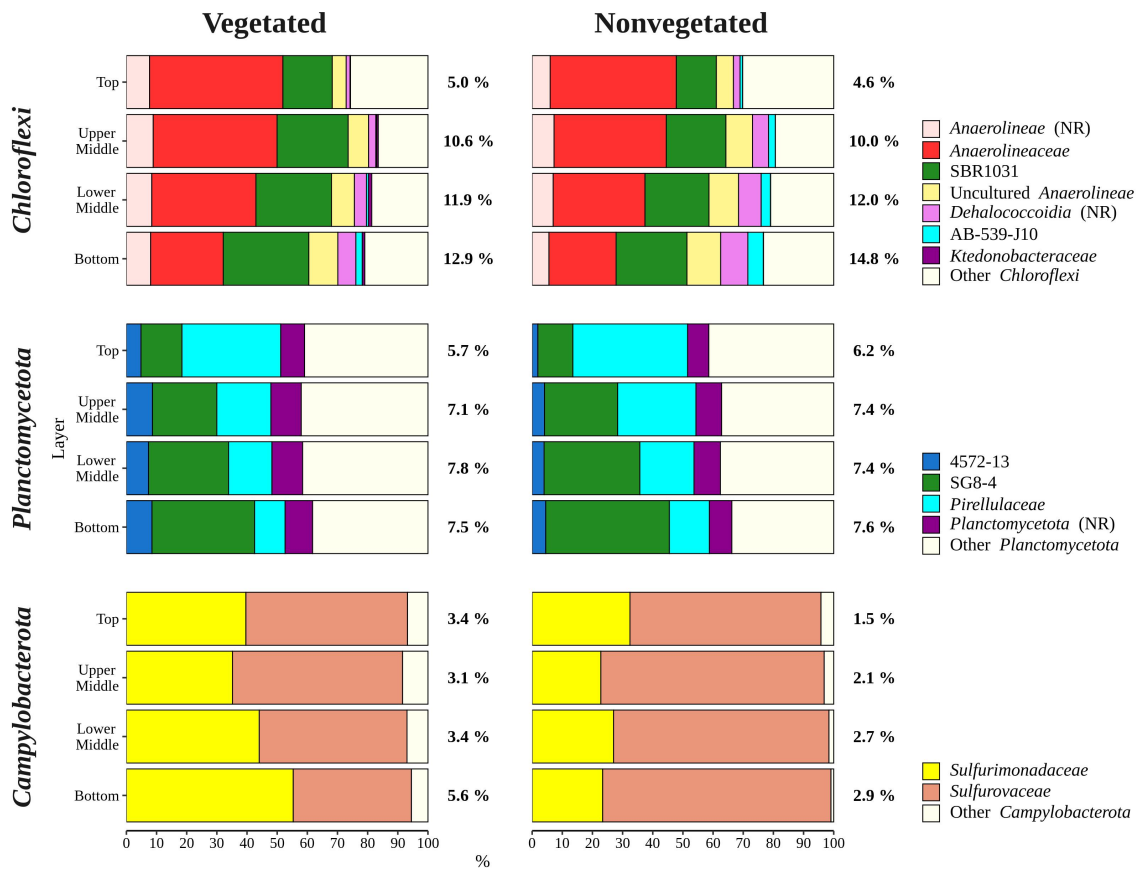


Figure 7. Taxonomic classification and relative contribution of the most abundant ($\geq 1\%$) taxonomic groups within *Chloroflexi*, *Planctomycetota*, and *Campylobacterota* in sediment communities sampled at the vegetated and nonvegetated site in the Bay of Saline. NR – sequences without known relatives